

Supporting Information

Sputtering deposition of gold nanoparticles onto graphene oxide functionalized with ionic liquids: biosensor materials for cholesterol detection

Nathália M. Galdino, Gabriele S. Brehm, Roberta Bussamara,* Wellington D. G. Gonçalves, Gabriel Abarca and Jackson D. Scholten*

Instituto de Química, UFRGS, Av. Bento Gonçalves 9500, Agronomia, CEP 91501-970, Porto Alegre-RS, Brazil.

Corresponding authors: roberta.bussamara@ufrgs.br; jackson.scholten@ufrgs.br (Tel: +55 51 3308 9633).

1. Experimental

1.1. General

The ILs were synthesized under argon atmosphere. All the reagents were purchased from commercial sources and used without purification. Cholesterol oxidase from microorganisms lyophilized powder (33 U/mg) and 4-aminoantipyrine reagent grade were purchased from Sigma Aldrich. Sodium phosphate monobasic anhydrous 98% P.A. (NaH_2PO_4) and sodium phosphate dibasic anhydrous P.A. (Na_2HPO_4) were achieved from Neon and were used for the preparation of phosphate buffer (pH 7.0).

1.2. Synthesis of the graphene oxide

The graphene oxide was prepared following a similar Hummer method previously reported.¹ This method consists of successive oxidation steps in order to separate the graphene oxide sheets.

1.3. Synthesis of amine-functionalized ionic liquids

1.3.1. Synthesis of 1-(3-aminopropyl)-1H-imidazol-3-ium bromide (IL 1)

The mono-amine-functionalized ionic liquid (IL 1) was synthesized by adapting a method already described.² In a typical synthesis, 1-methylimidazole (20 mmol) and 3-bromopropylamine hydrobromide (20 mmol) were mixed in ethanol (50 mL) and placed under reflux under argon atmosphere for 24 h. The resulting IL was purified by crystallization. This IL is soluble in DMF, ethanol, DMSO and water and it is stable under air. ¹H NMR (D₂O): δ = 8.74 (s, 1 H), 7.48 (s, 1 H), 7.42 (s, 1 H), 4.29 (t, J(H,H) = 7.2 Hz, 2 H), 3.02 (t, J(H,H) = 7.8 Hz, 2 H), 2.23 ppm (m, 2 H).

1.3.2. Synthesis of 1,3-bis(3-aminopropyl)imidazolium bromide (IL 2)

The IL containing two amine groups attached to the imidazolium cation was prepared by a synthetic method previously reported.³ In this case, potassium hydride (10 mmol, 0.24 g) was added to THF (8 mL) in an ice bath followed by the addition dropwise of a solution containing imidazole (10 mmol, 0.68 g) in THF (8 mL). The ice bath was removed and the solution was kept under stirring for 2 h at room temperature. Then, a solution of 3-bromopropylamine hydrobromide (20 mmol, 4.38 g) dissolved in THF (25 mL) was added slowly to the system. The mixture was kept under reflux for 12 h. After, the precipitate was washed with THF and dried under vacuum, resulting in a pale yellow solid. ¹H NMR (CDCl₃, 400 MHz): δ ppm 8.65 (s, 1 H), 7.43 (m, 2 H), 4.28 (t, 4 H), 4.16 (m, 4 H, CH₂), 2.70 (t, 4 H), 2.45 (m, 4 H).

1.4. Functionalization of graphene oxide with ionic liquids

The functionalization of graphene oxide with ionic liquids was performed according to a previous published procedure.⁴ After this process, the resulting material is usually called reduced graphene oxide (rGO). Typically, 100 mg of the graphene oxide was added to water (100 mL) and placed under ultrasound during 1 h affording a yellow solution. Then, IL (IL 1 or IL 2) (200 mg) was added to the solution, where it could be observed the formation of a gel. After, 200 mg of KOH was added to the solution, which was heated to 80 °C under vigorous stirring for 24 h. The materials were centrifuged, washed with HCl aqueous solution (10%) and ethanol and dried under vacuum oven.

1.5. Sputtering deposition of gold nanoparticles

The IL-GO samples were placed under vacuum for approximately 2 h at 298 K prior to its introduction in the sputter chamber as solid substrate for sputtering deposition of gold. All glassware used in the following procedures was cleaned in a bath of freshly prepared HNO₃/HCl (1:3, v/v), rinsed thoroughly in purified water, and dried prior to use. Deposition for 120 s was performed in a MED 020 (Bal-Tech) in the sputter mode with discharge voltage of 335 V (40 mA) under an argon pressure of 2 Pa at room temperature. In each deposition, a mass of 150 mg of IL-GO was placed on a Petri plate (3 cm in diameter) and set horizontally in the sputter coater. The solid surface was located at a distance of 50 mm from the gold target (99.9999% purity). After the deposition, the chamber was vented and the black solid was recovered and stored under argon for their further characterization and application.

1.6. TEM analysis

TEM analyses were carried out on an electron microscope at CMM-UFRGS operating at an accelerating voltage of 80 kV (JEOL JEM-1200 EXII). For these measurements, the supported Au nanoparticles were dispersed in 2-propanol, and a drop of the solution was spotted on a copper grid. The histogram of size distribution of the Au nanoparticles was obtained by using ImageJ and OriginPro softwares. For the histograms, around 300 nanoparticles were counted in different regions of the micrographs.

1.7. XPS analysis

For the XPS measurements, the Au NPs/IL-GO materials were pressed in order to produce pellets and were introduced into the SXS beamline endstation (LNLS).⁵ The samples were investigated using the long scan, Au 4f, N 1s, O 1s, and C 1s regions. The spectra were collected using an InSb(111) double-crystal monochromator at fixed photon energy of 1840 eV. The hemispherical electron analyzer (PHOIBOS HSA500 150 R6) was set at a pass energy of 30 eV, and the energy step was 0.1 eV, with an acquisition time of 200 ms/point. The overall resolution achieved was about 0.3 eV ($E_{ph} = 1840$ eV). The base pressure used inside the chamber was around 5.0×10^{-9} mbar. The monochromator photon energy calibration was done at the Si K edge (1839 eV). An

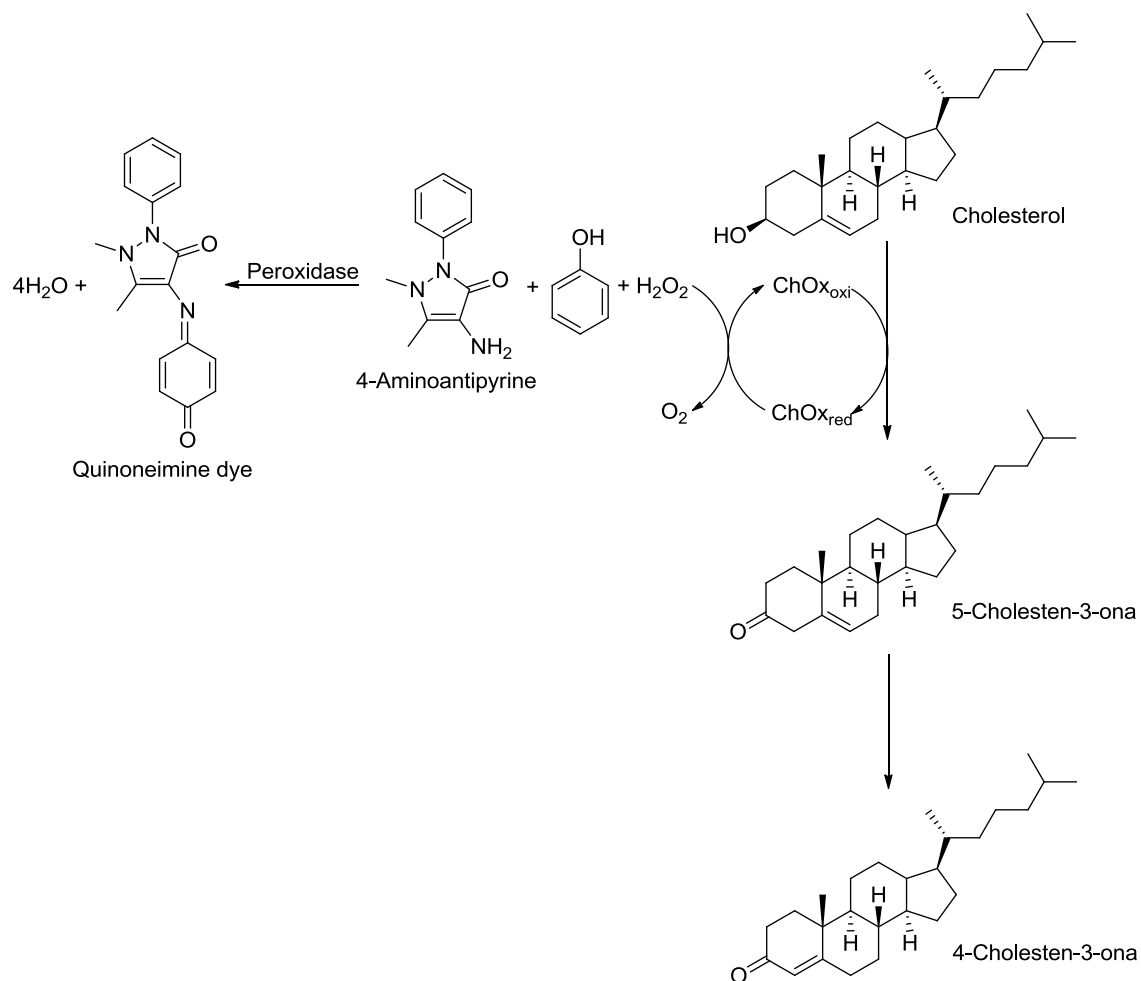
additional calibration of the analyzer energy was performed using a standard Au foil (Au 4f_{7/2} peak at 84.0 eV). The C 1s peak value of 284.6 eV (adventitious carbon) was considered as a reference to verify possible charging effects. The XPS measurements were obtained at a 45° take off angle at room temperature. CasaXPS program was used to fit the XPS results. All peaks were adjusted using a Shirley type background and an asymmetric Gaussian-Lorentzian sum function (with 30% Lorentzian contribution).

1.8. Cholesterol oxidase immobilization on the Au NPs/IL-GO materials

The enzyme immobilization was performed submerging the Au NPs/IL 1-GO or Au NPs/IL 2-GO (3 mg) in 0.5 mL of cholesterol oxidase solution (0.0015 U/mL in Na₂PO₄/NaHPO₄ buffer pH 7.0). The mixtures were kept at 4 °C during 24 h. As a control procedure, the graphene oxide (GO), graphene oxide with Au NPs (Au NPs/GO) and graphene oxide functionalized with ionic liquids (IL 1-GO and IL 2-GO) were tested with and without enzyme. After immobilization, unbounded ChOx was then drained out, and the support was washed (1x1.0 mL) with buffer solution in order to remove all unbounded ChOx from the support. Supernatants and washing buffers were tested for enzyme activity to determine indirectly the amount of enzyme immobilized on the support. The recovered activity after enzyme immobilization was quantified using the immobilized material to measure the ChOx activity as described in cholesterol oxidase activity assay section.

1.9. Detection of cholesterol by ChOx assay

The assay was performed by measuring the increase in absorbance at 500 nm in a UV-Vis spectrophotometer (Varian Cary 100 Con) caused by the oxidation of 4-aminoantipyrine as shown in Scheme S1.



Scheme S1 Pathways for the enzymatic measurement of cholesterol.

In order to analyze the linearity of enzyme response to cholesterol, different concentrations of cholesterol solutions (9.95, 19.8, 39.21, 58.25, 95.24 and 130.84 mg/L) were tested. The biosensors activities were measured according to a method previously reported with modifications.⁶ To initiate the reaction, 3 mg of ChOx-Au NPs/IL 1-GO or ChOx-Au NPs/IL 2-GO was mixed with 0.5 mL of buffer solution, 0.5 mL of color reagent (Na₂PO₄/NaHPO₄ buffer pH 7.0, phenol 28 mmol/L, peroxidase enzyme 800 U/L, 4-aminoantipyrine 0.5 mmol/L and sodium azide 15 mmol/L) and the solution containing cholesterol. The reaction mixture was kept at 37 °C for 1 h. The enzyme activity was analyzed in a UV-Vis spectrophotometer at 500 nm using a calibration curve (Table S1).

Table S1 Percentage of cholesterol oxidase immobilized on the materials and the recovered activity of biosensors comparing with free enzyme

Material	Percentage of ChOx immobilized on the supports ^a	Percentage of ChOx activity after immobilization ^b
Free ChOx	-	100%
ChOx-Au NPs/IL 1-GO	93%	76%
ChOx-Au NPs/IL 2-GO	92%	54%
ChOx-GO	73%	215%
ChOx-Au NPs/GO	73%	225%
ChOx-IL 1-GO	58%	42%
ChOx-IL 2-GO	54%	45%
GO	-	132%
Au NPs/GO	-	74%

^a Percentage of ChOx immobilized on the supports was calculated indirectly by comparing the quantity of enzyme added to the support with the amount of enzyme found at the supernatant and wash buffers.

^b Percentage of ChOx activity after immobilization was calculated by comparing the free enzyme activity with the immobilized enzyme activity using 19.8 mg/L of cholesterol solution.

1.10. Biosensing experiments in the presence of interferents

The tests in the presence of interferents were carried out similarly to total cholesterol detection. In the experiment, it was used 3 mg of ChOx-Au NPs/IL 1-GO or ChOx-Au NPs/IL 2-GO with 0.5 mL of buffer solution, 0.5 mL of color reagent ($\text{Na}_2\text{PO}_4/\text{NaHPO}_4$ buffer pH 7.0, phenol 28 mmol/L, peroxidase 800 U/L, 4-aminoantipyrine 0.5 mmol/L and sodium azide 15 mmol/L) and a solution containing the interferent in a regular blood concentration.⁷ The reaction mixture was kept at 37 °C for 1 h. The enzyme activity was analyzed in a UV-Vis spectrophotometer at 500 nm using a calibration curve. Then, cholesterol (19.8 mg/L) was added and the mixture was kept at 37 °C for 1 h and analyzed by UV-Vis.

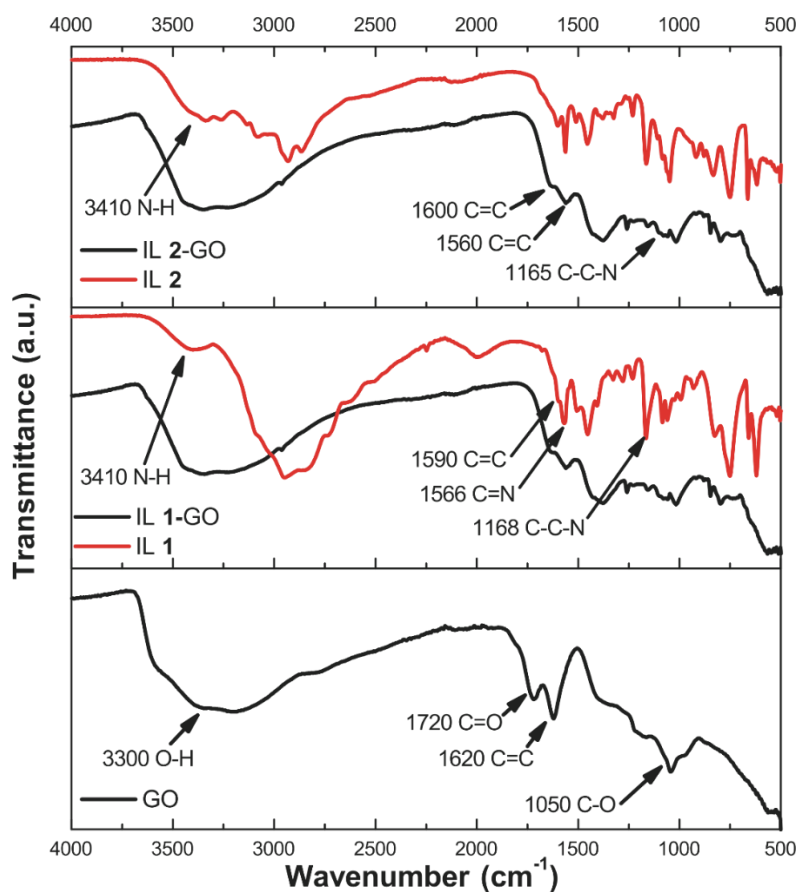


Fig. S1 FTIR analyses of the GO (bottom), IL 1-GO (middle) and IL 2-GO (top) materials.

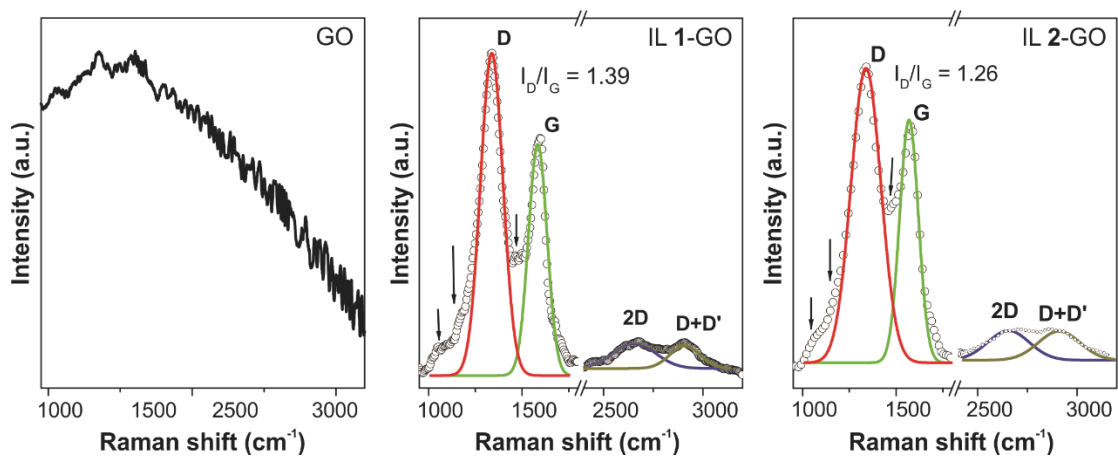


Fig. S2 Raman analyses of the GO, IL 1-GO and IL 2-GO. Black points represent the experimental data. Deconvolution of peaks was represented by D (red), G (green), 2D (blue) and D+D' (dark yellow), respectively. Arrows represent the covalent functionalization of the ionic liquids on the GO surface.

For the determination of the size of the graphite crystallite sites, the Tuinstra and Koenig relation was used (Equation 1).^{8, 9} The C_a constant was obtained through the empirical approximation⁸: $C_a = 160E_l^{-4}$ and E_l is the excitation energy of the laser.

$$L_a = C_a \cdot \left(\frac{I_D}{I_G}\right)^{-1} \quad \text{Equation 1}$$

L_a = crystallite size, I_D/I_G = intensity ratio between D and G signals, and C_a = constant dependent on laser energy (in this work: $E_l = 1.96$ eV (632.8 nm), then $C_a = 10.84$).

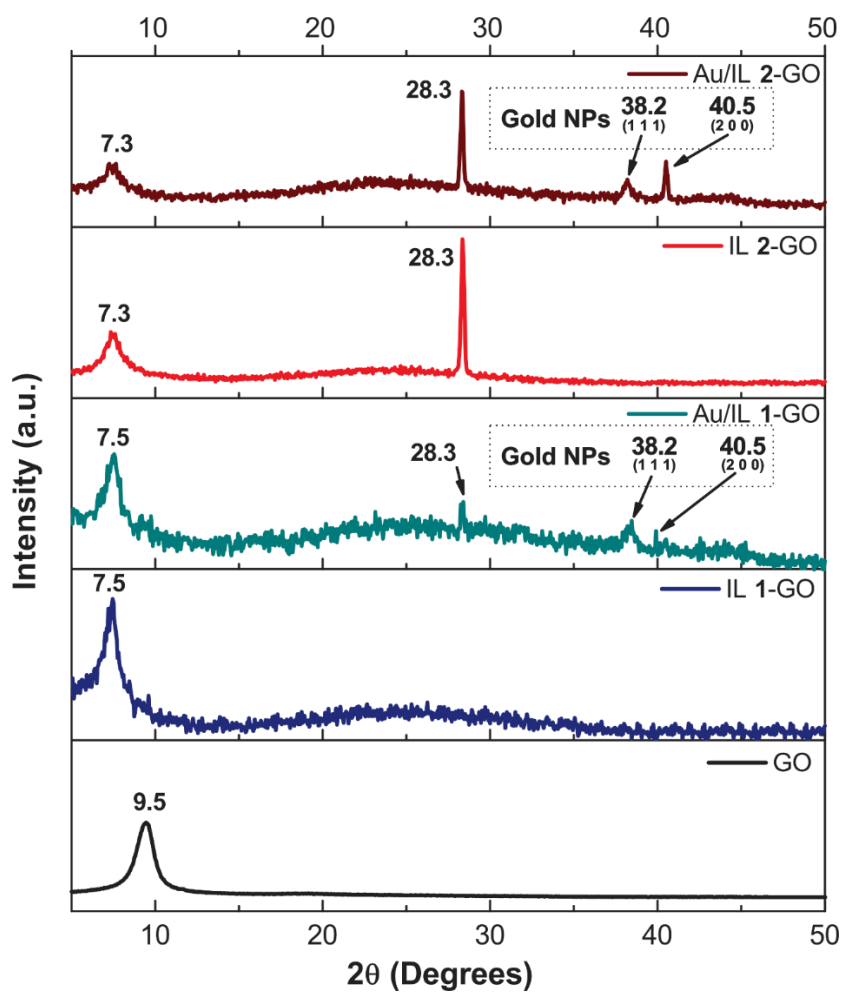


Fig. S3 XRD patterns obtained for GO, IL 1-GO, Au/IL 1-GO, IL 2-GO and Au/IL 2-GO materials.

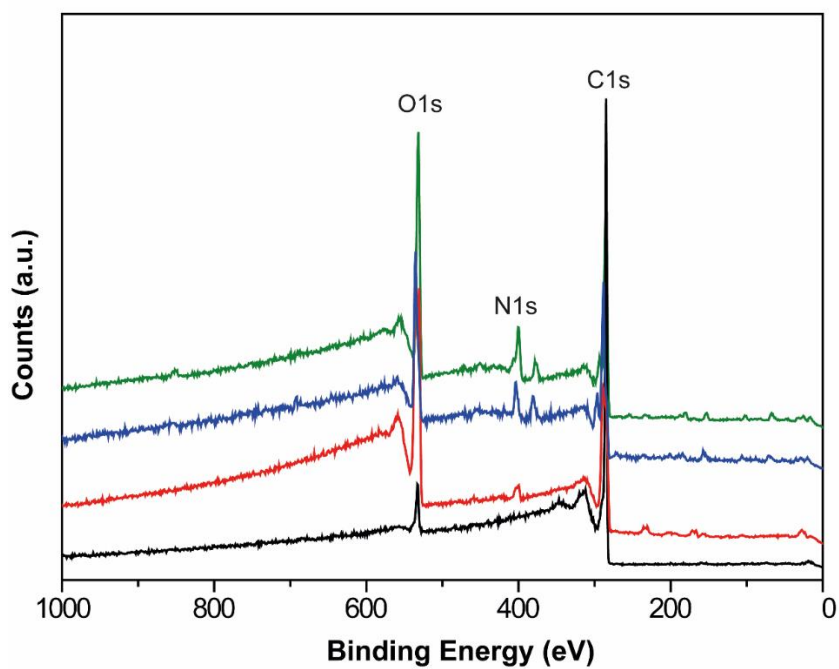


Fig. S4 XPS measurements at the long scan region. Black, red, blue and green solid lines represent graphite, GO, IL 1-GO and IL 2-GO, respectively.

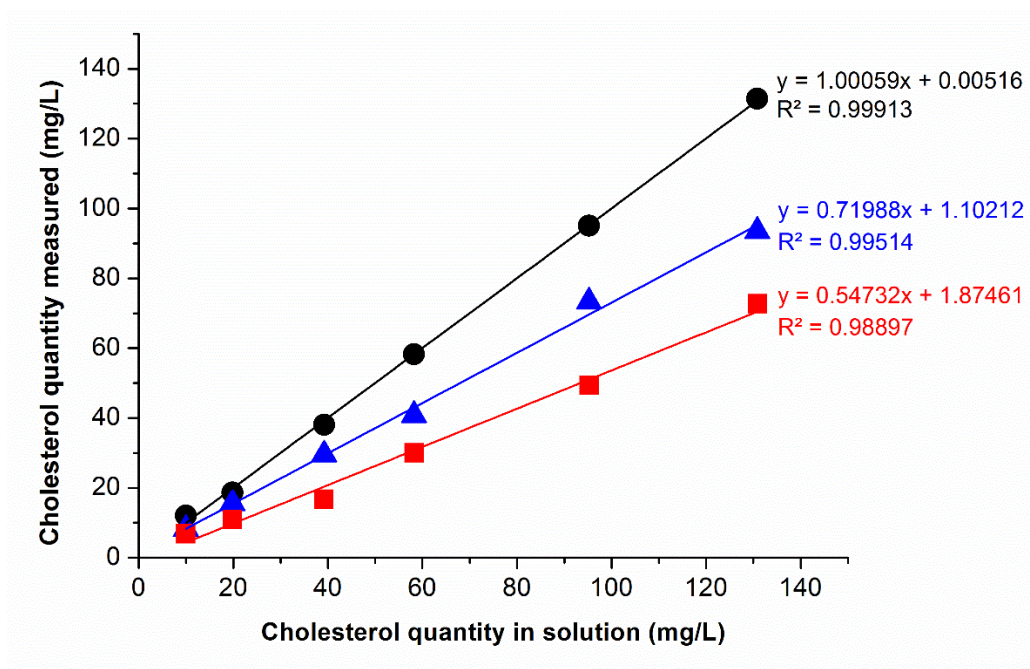


Fig. S5 Linear plot of total cholesterol detection by (■) free-ChOx, (●) ChOx-Au NPs/IL 1-GO and (▲) ChOx-Au NPs/IL 2-GO.

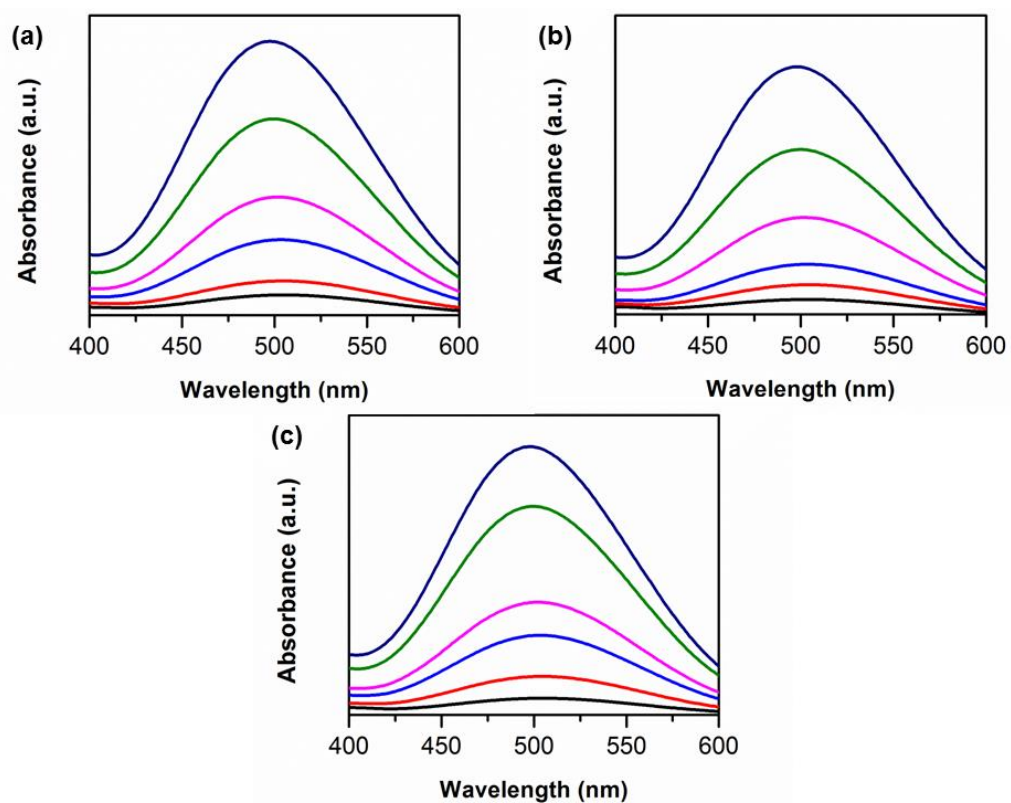


Fig. S6 UV-Vis spectra of total cholesterol detection at different concentrations: (—) 9.95, (—) 19.8, (—) 39.21, (—) 58.25, (—) 95.24 and (—) 130.84 mg/L using (a) free ChOx, (b) ChOx-Au NPs/IL 1-GO and (c) ChOx-Au NPs/IL 2-GO.

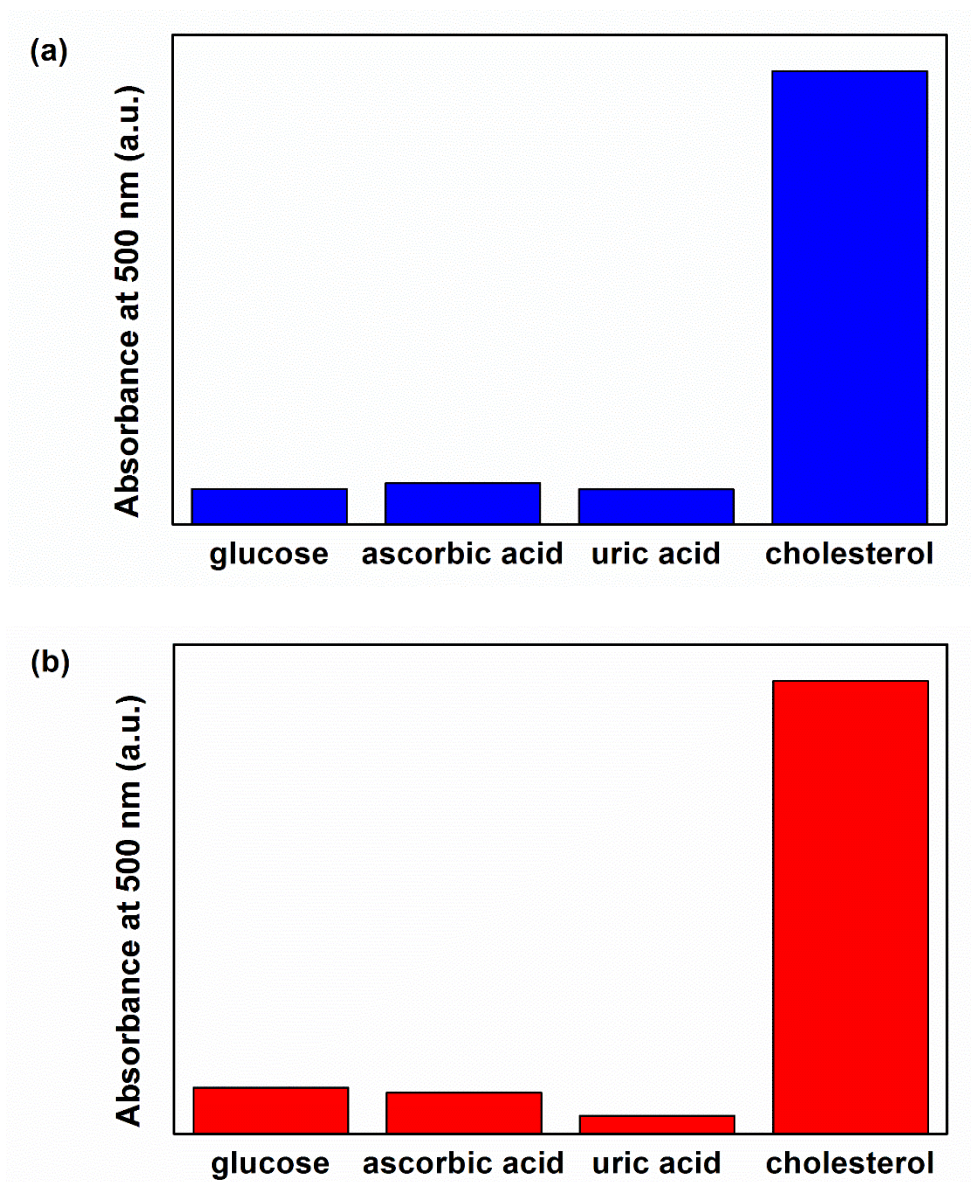


Fig. S7 Response of the hybrid materials in the presence of interferents (glucose 0.1 mmol/L, ascorbic acid 2.5 μ mol/L and uric acid 20 μ mol/L): **(a)** ChOx-Au NPs/IL 1-GO and **(b)** ChOx-Au NPs/IL 2-GO.

References

1. J. Wang, X.-B. Zhang, Z.-L. Wang, L.-M. Wang and Y. Zhang, *Energy Environ. Sci.*, 2012, **5**, 6885-6888.
2. Y. J. Zhang, Y. F. Shen, J. H. Yuan, D. X. Han, Z. J. Wang, Q. X. Zhang and L. Niu, *Angew. Chem. Int. Ed.*, 2006, **45**, 5867-5870.
3. C. Y. Li, J. F. Zhao, R. Tan, Z. G. Peng, R. C. Luo, M. Peng and D. H. Yin, *Catal. Commun.*, 2011, **15**, 27-31.

4. H. F. Yang, C. S. Shan, F. H. Li, D. X. Han, Q. X. Zhang and L. Niu, *Chem. Commun.*, 2009, 3880-3882.
5. H. Tolentino, V. Compagnon-Cailhol, F. C. Vicentin and M. Abbate, *J. Synch. Rad.*, 1998, **5**, 539-541.
6. C. C. Allain, L. S. Poon, C. S. G. Chan, W. Richmond and P. C. Fu, *Clin. Chem.*, 1974, **20**, 470-475.
7. S. Singh, P. R. Solanki, M. K. Pandey and B. D. Malhotra, *Anal. Chim. Acta*, 2006, **568**, 126-132.
8. L. G. Cançado, A. Jorio, E. H. M. Ferreira, F. Stavale, C. A. Achete, R. B. Capaz, M. V. O. Moutinho, A. Lombardo, T. S. Kulmala and A. C. Ferrari, *Nano Lett.*, 2011, **11**, 3190-3196.
9. F. Tuinstra and J. L. Koenig, *J. Chem. Phys.*, 1970, **53**, 1126-1130.